

Optical Manipulation of F-Actin with Photoswitchable Small Molecules

Malgorzata Borowiak,[#] Florian Küllmer,[#] Florian Gegenfurtner, Sebastian Peil, Veselin Nasufovic, Stefan Zahler, Oliver Thorn-Seshold, Dirk Trauner,^{*} and Hans-Dieter Arndt^{*}



Cite This: <https://dx.doi.org/10.1021/jacs.9b12898>



Read Online

ACCESS |



Metrics & More

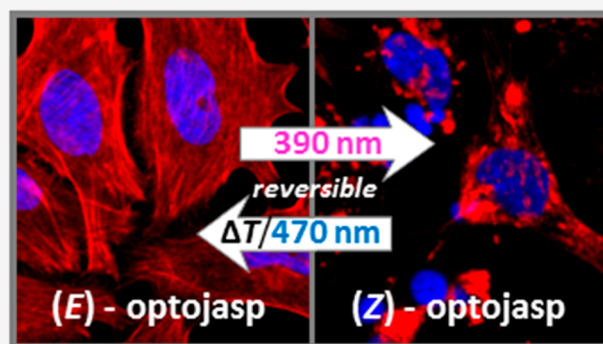


Article Recommendations



Supporting Information

ABSTRACT: Cell-permeable photoswitchable small molecules, termed **optojasps**, are introduced to optically control the dynamics of the actin cytoskeleton and cellular functions that depend on it. These light-dependent effectors were designed from the F-actin-stabilizing marine depsipeptide jasplakinolide by functionalizing them with azobenzene photoswitches. As demonstrated, **optojasps** can be employed to control cell viability, cell motility, and cytoskeletal signaling with the high spatial and temporal resolution that light affords. **Optojasps** can be expected to find applications in diverse areas of cell biological research. They may also provide a template for photopharmacology targeting the ubiquitous actin cytoskeleton with precision control in the micrometer range.



INTRODUCTION

Actin is the most abundant cellular protein and an essential component of the eukaryotic cytoskeleton.¹ Its ability to reversibly assemble into long supramolecular filaments² drives the definition of cell shape, migration, endocytosis, phagocytosis, and intracellular transport. In neurons, actin remodeling configures dendritic spines, is required for synapse function, and is a key component in axonal growth.³ In the nucleus, nuclear actin contributes to RNA transcription and chromatin maintenance.⁴ Actin also plays a critical role in cell division as an essential component during cytokinesis.⁵

The actin cytoskeleton is highly dynamic and undergoes constant remodeling in response to the physiological state and external stimuli. From a pool of a globular monomeric form (G-actin), a polymeric, filamentous form (F-actin) is generated, which dynamically interconverts through assembly and disassembly in an adenosine triphosphate (ATP)-dependent and -consuming process (“treadmilling”). F-Actin consists of two helically intertwined strands of a supramolecular protein polymer fiber that can be hierarchically arranged by actin binding proteins in parallel bundles, branched dendritic networks, and stress fibers, leading to diverse microfilament topologies of variable dynamics.¹

The key role of actin dynamics in living organisms has led to the evolution of interfering secondary metabolites,⁶ including the polyketides cytochalasin⁷ and latrunculin,⁸ as well as the (bi)cyclic peptides phalloidin (1), chondramide (2), and jasplakinolide (3, sometimes also referred to as “jaspamide”, Figure 1a).⁹ The cytochalasins and the latrunculins retard polymerization and enhance depolymerization by binding

tightly to the G-actin monomer.¹⁰ By contrast, phalloidin and jasplakinolide are incorporated at the interface between three actin subunits, promoting aggregation and suppressing depolymerization.¹¹ These small molecules and their derivatives have become powerful tool compounds for research.^{12,13} Fluorescent derivatives of phalloidin are common reagents for visualizing actin filaments in fixed cell microscopy.¹⁴ The silicon-rhodamine conjugate 4, termed SiR-actin, is cell permeable and images F-actin dynamics in living cells.¹⁵ SiR-actin is prepared by total synthesis and features an optimized jasplakinolide-derived structure¹⁶ that is more chemically stable (Figure 1b).

Although actin inhibitors have potent antimigratory activity and are toxic to cancer cells, systemic toxicity resulting from disturbed actin dynamics in healthy tissue has prevented them from reaching therapeutic application.¹⁷ Moreover, many actin-dependent processes are anisotropic and time-dependent,^{18,19} which limits the utility of globally acting inhibitors.^{6,12} Inhibitors that could instead be directed to modulate the actin cytoskeleton more precisely would circumvent these drawbacks and be extremely valuable for research and therapy.

Spatiotemporal control can be realized by incorporating photoswitches into bioactive molecules.^{20,21} Molecular photo-

Received: January 3, 2020



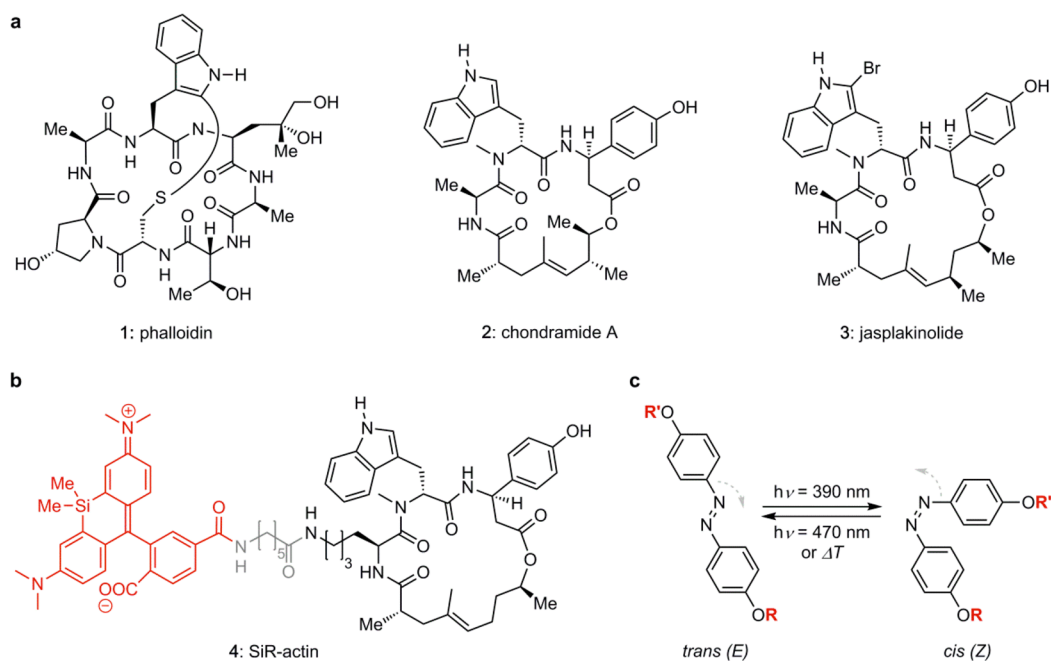


Figure 1. (a) Chemical structures of F-actin stabilizing natural products. (b) Structure of SiR-actin composed of the silico-rhodamine fluorophore (red), a linker (gray), and the optimized jasplakinolide scaffold (right). (c) Azobenzene isomerization controlled by illumination.

switches are particularly well suited to modulate dynamic, nonlinear processes, as featured in cytoskeleton biology, in G-protein coupled receptor pathways, and in neuronal signaling. Indeed, photopharmacology has been successfully used *in vivo* to control receptor signaling,²² tubulin dynamics,²³ and to restore visually guided behavior in blind animals.²⁴ Azobenzenes that show metastable irradiation-dependent change in their diazene configuration have been frequently applied in this regard (Figure 1c).^{24,25} Here, we introduce a family of azobenzene-based small molecules, termed **optojasps**, that provide direct optical control of the actin cytoskeleton.

Design and Synthesis of the Optojasps. For designing the **optojasps**, the noticeable dependence of cell permeability and actin-staining potential on fluorophore type and linker length of conjugates, such as **4**, was key.^{15,16} Without any specific mechanistic conjecture, it suggested that modulating the activity of jasplakinolides by placing an azobenzene in the same region as the fluorophore of **4** might be possible. Such an “azo-extension” strategy has been successful with ion channel blockers²⁶ and dihydrofolate reductase inhibitors.²⁷ For initial screening, a panel of eight **optojasps** was considered, which differed in the length of the connecting amino acid side chain (diaminopropionate, diaminobutyrate, ornithine, lysine) and in the geometry of the appended azobenzene photoswitch (Figure 2a). The latter were connected in *para* (azo-1, Figure 2c) or *ortho* (azo-2) in order to probe for different interactions exerted by the photoswitch in its respective *trans* or *cis* isomeric state.

The azobenzenes finally chosen featured 4,4'-dialkoxy substituents to ensure high bidirectional completion of photoswitching and retarded thermal isomerization. They were 3,4,5-trimethoxylated in the A-ring to improve solubility by disfavoring compound aggregation (Figure 2a,c).²³ Notably, while structurally related photostatin switches (e.g., **18**, Figure 2c) have been successfully used for targeting tubulin,²³ extensive structure–activity relationship (SAR) studies and successful prodrug designs of combretastatin analogues²⁸ as

well as recent high-resolution X-ray crystal structures of tubulin-bound combretastatin in *cis*- and *trans*-configuration²⁹ suggested that any protrusion from the B-ring significantly larger than the *para* methoxy group of azobenzene **18** (Figure 2c, highlighted) entirely abrogates affinity for tubulin. Therefore, “clean” actin-selective photoswitches were expected to result from conjugation of the extended azo-1 (**16**) or azo-2 (**17**) scaffolds.

The syntheses of **optojasps** then used six building blocks each (Figure 2c).^{15,16,30} In brief, β -tyrosine derivative **5** was immobilized on solid phase (**6**, Figure 2b) and was sequentially extended by solid phase peptide synthesis (SPPS) with *N*-Me-Trp building block **11**, one of the diamino building blocks **12a–12d**, and the unsaturated acid **13**, to give tripeptides **7a–7d** after cleavage from the resin. Esterification with alcohol **14** provided dienes **8a–8d**. Ring-closing metathesis with Grubbs’ second-generation catalyst **15** yielded the macrocyclic cyclo-depsipeptides **9a–9d** as *E*-configured cycloalkenes. After acid-mediated deprotection, the ammonium salts **10a–10d** were coupled to azobenzene carboxylic acids azo-1 (**16**) or azo-2 (**17**) and deprotected to afford **optojasps 1–8** (Figure 2b) in 10–20% overall yield.

Photochemical and Biological Evaluation. An initial evaluation of the photochemical properties of **optojasps 1–8** showed that all compounds were photoswitched *trans*→*cis* with deep violet and *cis*→*trans* with green light, reaching satisfactory photostationary ratios upon deep violet irradiation (*cis/trans* typically 10:1). They were fairly stable to spontaneous thermal *cis*→*trans* relaxation (Figure 3). The azo-1 derived photoswitches showed very slow thermal relaxation ($t_{1/2} \approx 36$ h), whereas azo-2 switches displayed a relaxation half-life of ~ 80 min in CH₃CN at 25 °C. Not unexpectedly, thermal relaxation was found accelerated under physiologically relevant conditions (37 °C, determined in aqueous buffer, see Figure 3g). Notably, photoswitching was fully reversible, and compounds remained chemically stable

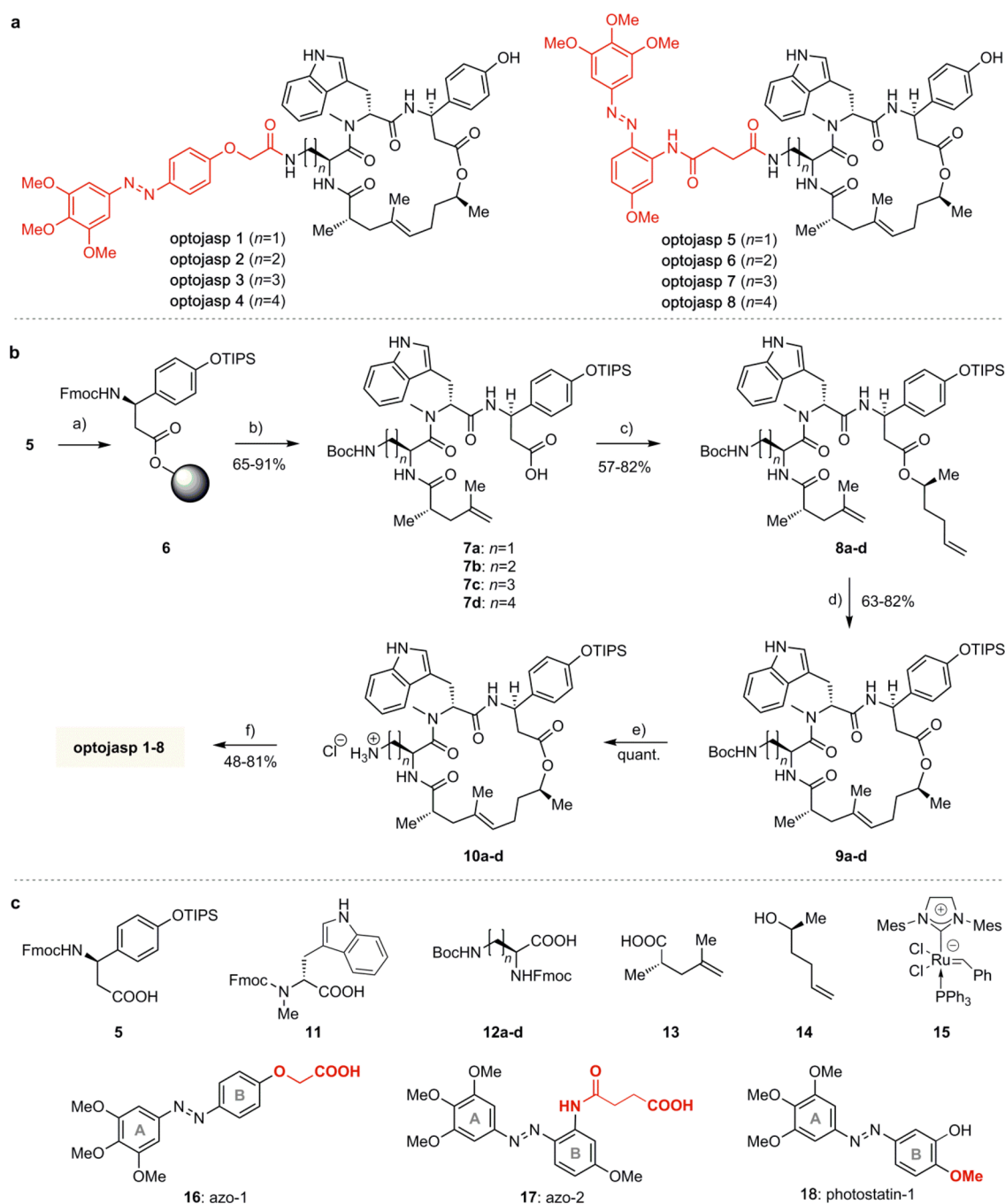


Figure 2. (a) Structures of **optojasps** 1–8. (b) Chemical synthesis of **optojasps**. Conditions: (a) 2-Chlorotrityl chloride resin, DIPEA, $\text{CH}_2\text{Cl}_2/\text{DMF}$; (b) 1. piperidine, DMF; 2. HATU, HOAt, 2, DIPEA, $\text{CH}_2\text{Cl}_2/\text{DMF}$; 3. piperidine, DMF; 4. HATU, HOAt, 12a, b, c, or d, DIPEA, $\text{CH}_2\text{Cl}_2/\text{DMF}$; 5. piperidine, DMF; 6. HATU, HOAt, 4, DIPEA, $\text{CH}_2\text{Cl}_2/\text{DMF}$; 7. HFIP, CH_2Cl_2 ; (c) EDCI, DMAP, DIPEA, 5, $\text{CH}_2\text{Cl}_2/\text{DMF}$; (d) catalyst 15, CH_2Cl_2 , rfx.; (e) 4 M HCl in dioxane, CH_2Cl_2 , 0 °C; (f) 1. 16 or 17, HATU, DIPEA, THF; 2. HF-pyridine, THF. (c) Building blocks used for **optojasp** synthesis and structure of tubulin-selective photostatin-1 (18). See text and [Supporting Information](#) for details.

even under prolonged (>12 h) pulsed irradiations with 390 and 450 nm light (Figure 3b and Figure S3).

Since membrane-permeant actin inhibitors are potent cytotoxins,¹² the **optojasps** were evaluated *in cellulo* for light-dependent cytotoxic activity in HeLa cells (Figure 3 and Figure S1). Multi-light-emitting diode (LED) arrays of a DISCO system²³ were used to deliver pulsed illuminations at different wavelengths. Notably, all **optojasps** were bioactive, indicating that the azo extension of the parent compound does neither compromise cell permeation nor compound binding. Compared to the dark-state *trans* isomers, most **optojasps** gained

potency upon illumination with 390 nm (*cis* form predominating; Figure 3g), while some stayed equipotent (**optojasps** 2 and 6). By contrast, the potency of **optojasps** 3 and 4 was higher in the dark (*trans*).

To investigate the mode of action and the selectivity of **optojasps** we investigated their effect on the cellular actin cytoskeleton by fluorescence microscopy (Figure 4). We observed that **optojasps** caused a light-dependent increase of actin nucleation, resulting in formation of large aggregates, and leading to very similar cellular phenotypes as caused by the F-actin stabilizers 1–3. HeLa cells exposed to the *cis*-active

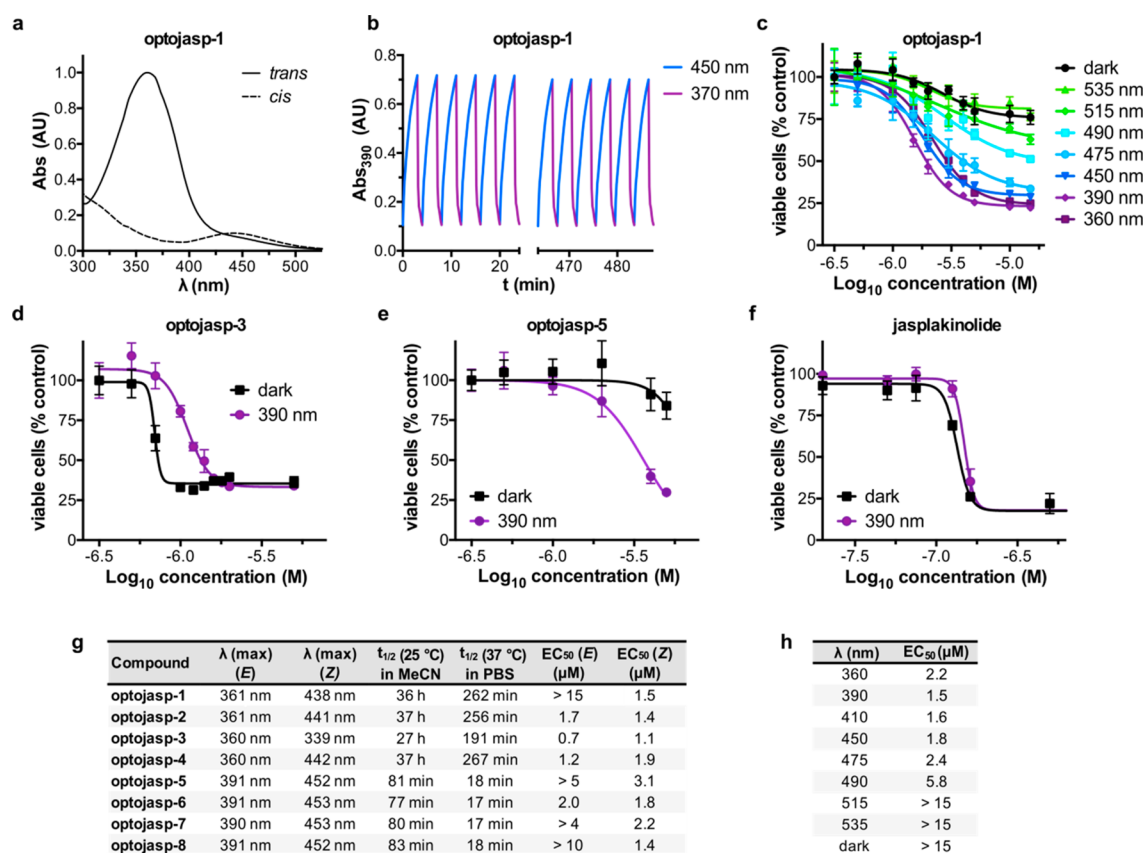


Figure 3. Switching properties and cytotoxicity of **optojasps**. (a) Absorption spectra of *cis* and *trans* **optojasp-1**. (b) Photoswitching reversibility monitored by absorption at 390 nm on pulsed treatment with 390 and 450 nm light. (c) Wavelength-dependent cytotoxicity of **optojasp-1** determined by MTT assay. (d–f) Photoswitching-dependent cell toxicity profiles for (d) “*trans*-active” **optojasp-3**, (e) “*cis*-active” **optojasp-5**, (f) jasplakinolide (**3**). (g) Photophysical and cytotoxicity parameters for **optojasps 1–8**, see Figure S1 for details. (h) Wavelength-dependent cytotoxicity of *cis*-active **optojasp-1**, related to panel (a). All data were obtained with HeLa cells (45 h, pulsed illuminations of 75 ms every 15 s at the specified wavelength or in the dark).

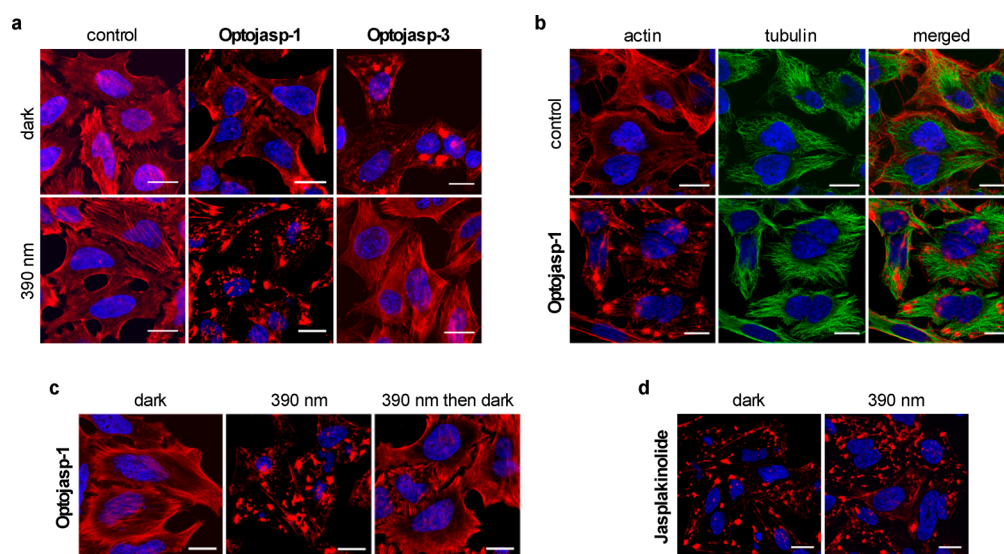


Figure 4. Light-dependent selective disruption of the actin cytoskeleton by **optojasps**. (a) HeLa cells treated with **optojasps** (1 μ M) in the absence or presence of 390 nm illumination, stained for F-actin (red). (b) HeLa cells untreated or treated with **optojasp-1** (1 μ M) in the absence or presence of 390 nm illumination, stained for tubulin (green). (c) Cells treated with **optojasp-1** (3 μ M) and exposed to 390 nm light for 5 h (“390 nm”), subsequently exposed to 475 nm light for 1 h, then kept in darkness for 12 h (“390 nm then dark”). (d) HeLa cells treated with jasplakinolide (**3**, 100 nM) for 5 h in the absence or presence of 390 nm irradiation. Nuclear DNA was stained with Hoechst 33342 (blue), cells were imaged after fixation, scale bar 20 μ m.

optojasp-1 showed induction of actin polymerization into amorphous clumps under 390 nm illumination, while cells maintained in the dark showed no abnormalities in the F-actin network. In line with the photophysical data, the *trans*-active **optojasp-3** displayed an inverted light dependency with actin cytoskeleton disruption occurring in the dark and with no effect on the organization of the F-actin network under 390 nm illumination (Figure 4a). By contrast, the microtubule network was clearly not affected by **optojasp-1** treatment (Figure 4b), even though the trimethoxy azobenzene motif is found in microtubule-disrupting photostatin photoswitches²³ and resembles a substructure motif of the tubulin-polymerization inhibitors colchicine and combretastatin A4.²⁸ Our data show that, by extending the **optojasp** switches at the combretastatin-like B-ring in *para*, affinity for tubulin is abrogated and that actin-selective conjugates for cytoskeleton disruption are obtained.

Incubation under actin-nucleating illumination conditions (**optojasp-1** with 390 nm light pulses over 5 h) led to a hyper-aggregated actin cytoskeleton (Figure 4c). Subsequent irradiation with light that promotes back-isomerization (475 nm pulse block for 1 h) followed by incubation in the dark for 10 h to further promote back-isomerization phenotypically recovered the regular actin cytoskeleton structure (Figure 4c).

To study whether the observed activities were connected to nonspecific interactions, we studied the physicochemical properties of the best candidate **optojasp-1** as well as its activity on target. Compound solubility remained unaffected by irradiation, that is, both *trans*- and *cis* form of **optojasp-1** were equally soluble. Furthermore, by collecting light-scattering data at 800 nm wavelength, we could not find any indication for compound aggregation in either *cis*- or *trans*-configuration (see Supporting Information for details).

On-target activity was then studied by measuring the rate of F-actin polymerization induced by **optojasp-1**, depending on its configurational state, using pyrene-labeled actin (Figure 5).³¹ We found that both forms of **optojasp-1** stimulated F-actin polymerization, but, to a lesser extent than jasplakinolide. Furthermore, the *cis* form of **optojasp-1** was found significantly more active than the *trans* form. Both observations are in good agreement with the cytotoxicity data.

By contrast, the azobenzene extensions **16** or **17** (not shown) devoid of the actin-binding ligand were incapable of promoting F-actin polymerization and did not modify the activity of jasplakinolide, neither in *cis* nor in *trans* form (see Supporting Information). These data strongly suggest that it is the direct molecular interaction of the **optojasps** with the F-actin target that accounts for their properties.

With target selectivity and reversibility established, we evaluated the potential of **optojasps** for photocontrol of cellular dynamics. Actin reorganization is involved in neuronal development and plasticity,³² cell cycle and division,¹⁹ as well as cell motility, invasive migration,¹⁸ and endocytosis.³³ When studying cell morphology, we observed that, upon irradiation with 390 nm, **optojasp-1** caused cells to detach rapidly from their substrate at doses that caused no morphological changes in the dark (Figure 6a, Movie 1, and Movie 2). Motile cells exposed to **optojasp-1** immediately stopped migrating upon illumination with 390 nm, reduced lamellipodia formation, and finally rounded up. We then performed cell tracking experiments to quantify the control of cell motility by photo-switching **optojasps**. In line with the phenotypic observations,

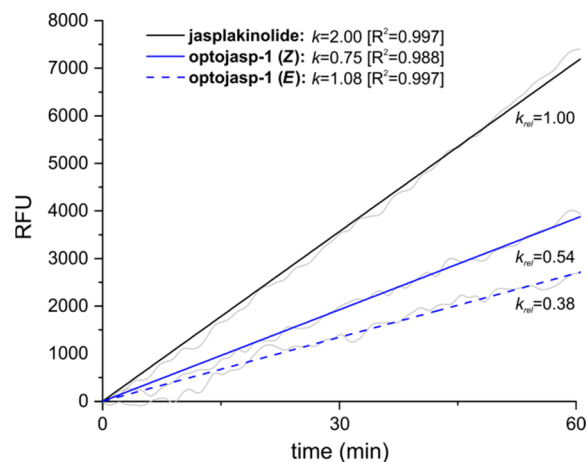


Figure 5. Illumination-dependent capacity of **optojasp-1** for inducing actin-polymerization *in vitro*. *trans*-**Optojasp-1**, *cis*-**optojasp-1**, or jasplakinolide (**3**, 20 μ M each) were incubated with pyrene-labeled actin (5 μ M) under low salt, nonpolymerizing conditions.³¹ Polymerization was monitored by pyrene fluorescence emission measurement at $\lambda_{Em} = 410$ nm after low-intensity excitation at $\lambda_{Em} = 350$ nm in 60 s intervals over 4 h at 37 $^{\circ}$ C. **Optojasp** configuration remained stable under these conditions (see Figure S5). Data are shown for the initial linear phase (1 h). All measurements were performed in duplicates in 384-well plates. RFU: relative fluorescence units, detector response normalized to fluorescence of pyrene-labeled G-actin in nonpolymerizing buffer. External fluorophore **16** was added to **3** to correct for azobenzene absorbance; k : slopes of linearly fitted curves in RFU/s; k_{rel} : comparative potential for induction of actin polymerization, normalized to jasplakinolide ($k_{rel} = 1$).

cell velocity and migration distance were found significantly reduced in a dose-dependent manner upon activation with 390 nm light. *cis*-Active **optojasps** were particularly robust in this application, reducing motility threefold in light-targeted cells only minutes after illumination, at doses where cells remained unaffected in the dark (Figure 6b, Movie 3, and Movie 4).

We also examined whether **optojasps** could optically control cell division, since its successful completion relies on proper chromosome segregation and correct functionality of the actin contractile ring.^{5,19} At intermediate doses **optojasp-1** was indeed capable of controlling the completion of cell division. While cell division proceeded with chromosome segregation to the state of daughter cell constriction, photoswitching stalled the separation of daughter cells. This blockade finally resulted in their refusion into tetraploids, strongly indicative of a dysfunctional contractile ring (Figure 6c, Movie 5, and Movie 6). These phenotypic data independently confirm that tubulin assembly remains unaffected by **optojasps**, which exert selective activity on F-actin dynamics only.

Furthermore, we investigated the ability of the **optojasps** to optically control processes acutely coupled to cytoskeletal signaling.³⁴ The myocardin-related transcription factor A (MRTF-A) was selected as an example, as it directly communicates changes of cytoplasmic actin dynamics to gene regulation.³⁵ G-Actin-bound MRTF-A is released when F-actin is formed. Liberated MRTF-A translocates into the nucleus, where it activates target genes depending on serum response factor (SRF).³⁶ We first used a fluorescent MRTF-A fusion protein in order to monitor its cellular localization. Indeed, upon treatment with activated **optojasps**, MRTF-A localized to the nucleus, just as observed after treatment with

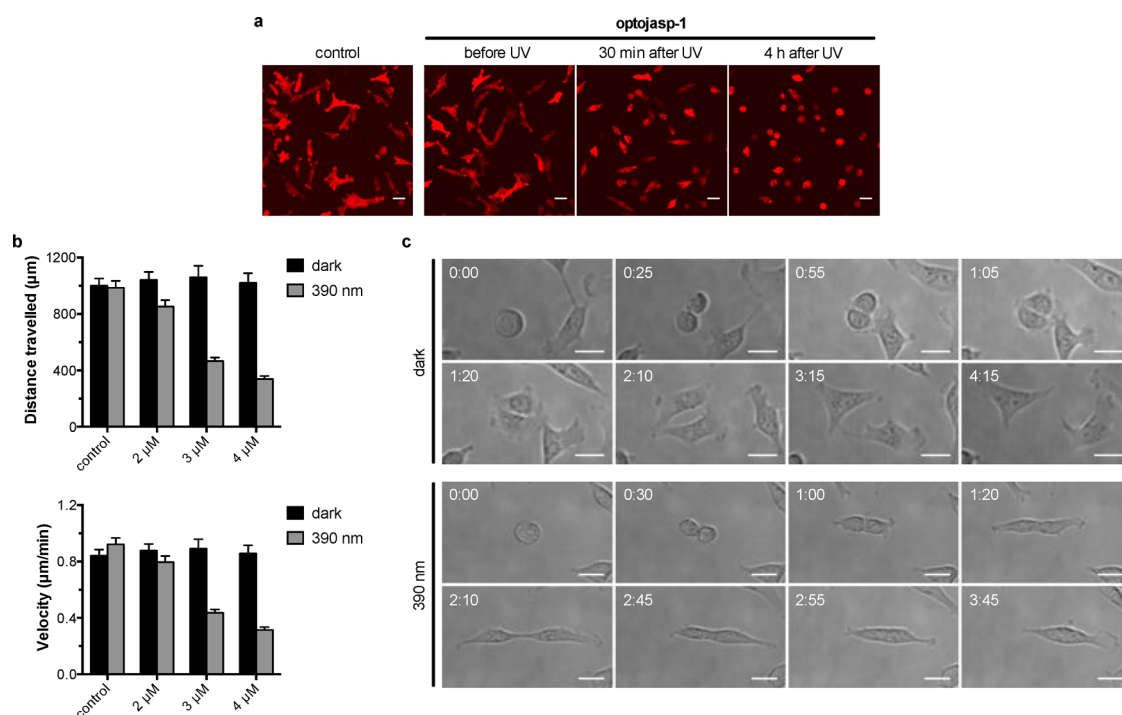


Figure 6. Optical control over cell shape, motility, and division. (a) Motile cells exposed to **optojasp-1** (5 μM) before and after illumination with 390 nm, see [Movie 1](#) and [Movie 2](#). (b) Quantification of light-dependent cell motility parameters with escalating doses of **optojasp-1**, see [Movie 3](#) and [Movie 4](#). (c) Dividing cells treated with **optojasp-1** (2.5 μM) in the dark or under 390 nm illumination, see [Movie 5](#) and [Movie 6](#). All experiments were conducted using MDA-MB-231 cells stably expressing mCherry-Lifeact; scale bars 40 μm , time shown as hh:mm. See [Supporting Information](#) for experimental details.

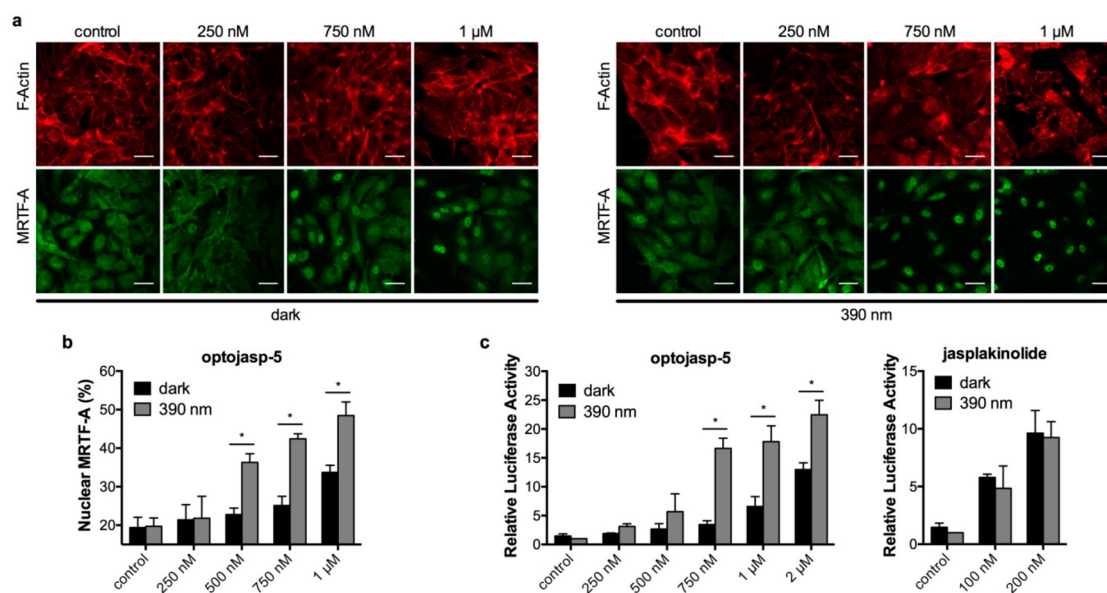


Figure 7. Optical control over MRTF-A signaling in human umbilical vein endothelial cells (HUVECs). (a) Cells expressing mCherry labeled MRTF-A exposed to escalating doses of **optojasp-5** in the dark or with 390 nm irradiation, stained for F-actin, and imaged after fixation. Scale bars 40 μm . (b) Quantification of the nuclear fraction of MRTF-A. (c) Dual luciferase reporter gene assay for SRF response elements in cells incubated with **optojasp-5** or **jasplakinolide**. Luciferase reporter activity is expressed in relative luminometer units (RLU) normalized to the constitutive renilla luciferase expression level (control). Bar graph results are given as mean \pm standard deviation (SD); statistical significance was determined by unpaired Student *t*-test, $p \leq 0.05$. See [Supporting Information](#) for details.

jasplakinolide. We selected **optojasp-5** for quantitative analysis, as this compound has a spontaneous *cis-trans* relaxation rate in the order of the biological response (18 min, [Figure 3](#)) and only a marginally lower efficacy compared to the slowly relaxing **optojasps-1–4**. Without

illumination, labeled MRTF-A remained homogeneously distributed in the cytoplasm ([Figure 7a](#)). When cells were exposed to **optojasp-5** and to 390 nm light, nuclear translocation of MRTF was significantly enhanced when compared to nonilluminated cells ([Figure 7a](#)). The effect was

most prominent at intermediate concentrations (250–750 nM).

Quantification of the nuclear fraction of MRTF-A confirmed the significance of these data (Figure 7b). These results indicate that MRTF-A can be specifically activated by **optojasp** photocontrol, further validating F-actin assembly as the direct **optojasp** target.

In addition, we studied the function of MRTF-A induction by using a luciferase reporter gene regulated by SRF. Cells treated with **optojasp-5** fully induced reporter gene expression, with strong optical control in the medium concentration range (Figure 7c). Jasplakinolide-treated control cells carrying the same reporter displayed strong, but illumination-independent, induction of luciferase activity upon compound treatment.

Finally, we investigated **optojasps**' ability to exert both time- and cell-specific control over actin-dependent processes in cellulo. After illumination bursts were delivered to regions of interest (ROIs) comprising single selected cells within a cell population, cellular response was individually monitored. For this experiment the slowly relaxing **optojasp-1** worked again well (Figure 8, Movie 7, and Movie 8). We reproducibly

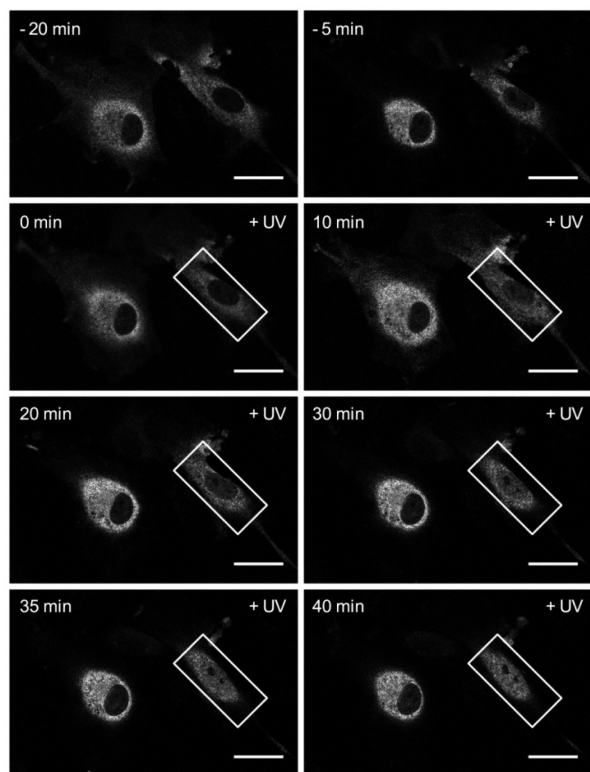


Figure 8. Time-lapse imaging series of MRTF-A:mCherry-expressing HUVEC cells following treatment with 750 nM **optojasp-1** and cell-specific, localized illumination (+UV, white rectangle ROI, 405 nm irradiation). Scale bars 20 μ m.

observed that light activation triggered actin-dependent MRTF-A translocation to the nucleus in exactly the defined ROI, with cell-by-cell spatial control applied side-by-side. The response that was both stable and rapid, and cross-talk to neighboring cells, was not observed. In nonilluminated cells, MRTF-A remained in the cytosol. Recovery was not evident on the time scale of the experiment, probably because stimulated F-actin aggregation needs longer time to recover (cf. Figure 4c). Nevertheless, these data strongly suggest that

optojasps directly work on F-actin as target and are capable of acutely blocking actin dynamics on the minute time scale with high spatial precision.

Taken together, our data show that **optojasps** are a robust and powerful tool to optically control the actin cytoskeleton and processes that depend on it. They can be used noninvasively in live cells, with exquisite spatial and temporal precision at the cellular level, and enable optical control over actin nucleation and cytotoxicity in cells, as well as over cell motility and cytoskeletal signaling.

DISCUSSION

Optical control of biological activity by using caged compounds, optogenetics, and more recently photopharmacology has advanced significantly in recent years. Photouncaging is by now routinely applied for spatiotemporal control in biology, particularly in neuroscience, where caged neurotransmitters are standard tools.³⁷ However, to our knowledge, reversibly controllable actin modulators have not yet been introduced for biological studies.

Precision control of cytoskeleton-associated proteins with light has been recently demonstrated by using optogenetics involving proteins that indirectly act on the actin cytoskeleton.^{38–40} On the one hand, engineering actin itself has been rather difficult due to the strong influence even small modifications have on its proper functioning. On the other hand, small-molecule photoswitches for the direct optical control of the microtubule cytoskeleton by tubulin polymerization inhibition have been developed^{23,41} and have already led to applications in neuroscience, morphogenesis, and *in vivo* applications in embryology.^{42–44} Photoswitchable tubulin stabilizers were recently reported as well.⁴⁵ By analogy, we expect that the small-molecule **optojasps** introduced here as photoswitchable F-actin modulators will provide a powerful tool for studying actin biology in a spatiotemporally controlled manner. In particular, we surmise that the ability to easily phototune the inhibitory activity of the **optojasps** by varying the wavelength of illumination (“photodosing”, Figure 3) to sensitively set the isomer ratio above or below its activity threshold offers a robust and adaptable method for complex biological experiments, which is particularly advantageous when compared to irreversible photouncaging approaches.

Optojasps retain most of the potency of the parent compound jasplakinolide and can be expected to bind to the same binding site on F-actin, considering all functional and phenotypic data acquired. However, the discovery of both *cis*-active and *trans*-active compounds alongside with compounds with barely photoswitchable bioactivity is intriguing considering their rather similar chemical structures. It suggests a specific molecular interaction of the **optojasps** with their target that directly involves the configurationally bistable azobenzene.

The **optojasp** design is based on an azo-extension of the jasplakinolide structural scaffold. Recent structure elucidations of F-actin bound with jasplakinolide and its Lys analogue by using cryo-electron microscopy showed that both bind at regular intervals inside the F-actin filament contacting three adjacent actin subunits.^{46,47} They reinforce the fiber by stabilizing a state of partial ATP hydrolysis that is only transient during regular F-actin turnover.⁴⁷ Interestingly, the lysine side chain of the bound analogue projects toward the interior of F-actin and extends into an inner cavity of moderate volume that is open to the outside (see Figure S2).

The macrocycle's binding pose can be expected to be retained for jasplakinolide conjugates. The azo-extension will then interact with the interior of the cavity and affect the affinity of the **optojasps** to F-actin. As the space in this cavity is confined, the ability to stabilize the F-actin fiber would become dependent on switch topology and its configuration. Such a model could tentatively explain the "switchability" and the ability to generate "cis-active" (**optojasp-1**) and "trans-active" modulators (**optojasp-3**), which would result from the individually different **optojasp** topologies and conformational preferences. Furthermore, altered conformational preferences of the **optojasp** macrocycle could contribute to switchability as well.

By contrast, changes in general compound properties are likely not strongly contributing to compound activity. Our experiments showed that solubility does not depend on switch configuration; neither was aggregation observed. While not investigated for all **optojasps** in detail, the single cell irradiation experiments conducted for studying MRTF-A signaling (Figure 8) as well as experiments with pre-irradiated compounds (data not shown) indicated that both the active and the inactive state should have comparable cell permeability. If this was not the case, local concentration reached by irradiation would probably be insufficient for observing any compound activity localized in the extremely small volume of a single cell ($\sim 10^{-14}$ m³). Furthermore, "spilling" of activity to neighboring cells, indicative of a highly diffusible active state populated by irradiation, was also not observed during these experiments. Finally, if the azobenzene configuration (*cis* or *trans*) would generally affect cell permeability, a concordant activity profile for all **optojasps** should emerge *in cellulo*—which is not the case. Together with the F-actin polymerization experiment, which supported direct on-target activity, these data strongly suggest that a direct structural interaction of the switch with the binding cavity is likely eliciting the observed properties.

CONCLUSION

Further mechanistic characterization and functional optimization notwithstanding, we expect that **optojasps** will become highly useful research tools for deciphering the complex role of actin in cell biology with the high temporal and spatial resolution that only light can provide. Importantly, our experimentation showed that switching the activity of the **optojasps** results in highly localized, acute activity on F-actin. This activity can be confined to a single cell. Since actin is highly conserved among all eukaryotes, the **optojasps** should be applicable in a variety of cell types originating from different organisms, provided they can be illuminated appropriately. Lastly, the **optojasps**' ability to inhibit actin dynamics only in selected cells could open new vistas for functional research in cancer biology and neuronal regeneration. **Optojasps** should hence prove a versatile and powerful tool for enabling high-precision cytoskeletal control inaccessible to other methods.

ASSOCIATED CONTENT

Supporting Information

The Supporting Information is available free of charge at <https://pubs.acs.org/doi/10.1021/jacs.9b12898>.

MTT assays, binding pocket region in F-actin, extended photoswitching stability trace of **optojasp1**, raw data of F-actin polymerization experiments, isomerization stabil-

ity monitoring, materials and methods including solubility and aggregation data, chemical synthesis and characterization, **optojasp** HPLC traces, ¹H NMR spectra, UV-vis spectra (PDF)

Movie 1. Cell morphology, **optojasp-1** in the dark (AVI)

Movie 2. Cell morphology, **optojasp-1** upon UV exposure (AVI)

Movie 3. Cell migration, **optojasp-1** in the dark (AVI)

Movie 4. Cell migration, **optojasp-1** upon UV exposure (AVI)

Movie 5. Cell division, **optojasp-1** in the dark (AVI)

Movie 6. Cell division, **optojasp-1** upon UV illumination (AVI)

Movie 7. MRTF nuclear translocation, UV illumination control (AVI)

Movie 8. MRTF nuclear translocation, **optojasp-5** with local UV exposure (AVI)

AUTHOR INFORMATION

Corresponding Authors

Dirk Trauner – Department of Chemistry, New York University, New York 10003 New York, United States; orcid.org/0000-0002-6782-6056; Email: dirktrauner@nyu.edu

Hans-Dieter Arndt – Institute for Organic Chemistry and Macromolecular Chemistry, Friedrich-Schiller-University, Jena D-07743, Germany; orcid.org/0000-0002-0792-1422; Email: hd.arndt@uni-jena.de

Authors

Malgorzata Borowiak – Department of Pharmacy, Ludwig-Maximilians University, München D-81377, Germany

Florian Küllmer – Institute for Organic Chemistry and Macromolecular Chemistry, Friedrich-Schiller-University, Jena D-07743, Germany

Florian Gegenfurtner – Department of Pharmacy, Ludwig-Maximilians University, München D-81377, Germany

Sebastian Peil – Institute for Organic Chemistry and Macromolecular Chemistry, Friedrich-Schiller-University, Jena D-07743, Germany

Veselin Nasufovic – Institute for Organic Chemistry and Macromolecular Chemistry, Friedrich-Schiller-University, Jena D-07743, Germany

Stefan Zahler – Department of Pharmacy, Ludwig-Maximilians University, München D-81377, Germany; orcid.org/0000-0002-5140-7287

Oliver Thorn-Seshold – Department of Pharmacy, Ludwig-Maximilians University, München D-81377, Germany; orcid.org/0000-0003-3981-651X

Complete contact information is available at: <https://pubs.acs.org/10.1021/jacs.9b12898>

Author Contributions

#M.B. and F.K. contributed equally.

Notes

The authors declare no competing financial interest.

ACKNOWLEDGMENTS

This research was supported by the National Institutes of Health (R01 GM126228 to D.T.), the Deutsche Forschungsgemeinschaft (SFB1032 to D.T., O.T.-S., and S.Z.; SFB152 and Emmy Noether grant to O.T.-S.), and the TMWWDG (Grant No. 43-5572-321-12040-12 to H.-D.A.). H.-D.A. is a PI

in the DFG-funded cluster of excellence “Balance of the microverse” (EXS 2051). M.B. was supported by LMU-Excellent (postdoctoral fellowship), V.N. by the DAAD (predoctoral fellowship), and S.P. by the GDCh (Hofmann-fellowship). We thank M. Reynders for help with synthesis and discussions, L. de la Rosa for help with cell biology, A. Akhmanova (Utrecht Univ., NL) for donating mCherry-Lifeact MDA-MB-231 cells, and the microscopy platform CALM for imaging support.

REFERENCES

- (1) Pollard, T. D.; Borisy, G. G. Cellular Motility Driven by Assembly and Disassembly of Actin Filaments. *Cell* **2003**, *112*, 453–465.
- (2) Dominguez, R.; Holmes, K. C. Actin Structure and Function. *Annu. Rev. Biophys.* **2011**, *40*, 169–186.
- (3) Papandreou, M.-J.; Leterrier, C. The Functional Architecture of Axonal Actin. *Mol. Cell. Neurosci.* **2018**, *91*, 151–159.
- (4) Eustermann, S.; Schall, K.; Kostrewa, D.; Lakomek, K.; Strauss, M.; Moldt, M.; Hopfner, K.-P. Structural Basis for ATP-dependent Chromatin Remodelling by the INO80 Complex. *Nature* **2018**, *556*, 386–390.
- (5) Glotzer, M. The Molecular Requirements for Cytokinesis. *Science* **2005**, *307*, 1735–1739.
- (6) Allingham, J. S.; Klenchin, V.; Rayment, A. I. Actin-Targeting Natural Products: Structures, Properties and Mechanisms of Action. *Cell. Mol. Life Sci.* **2006**, *63*, 2119–2134.
- (7) Katagiri, K.; Matsuura, S. Antitumor Activity of Cytochalasin D. *J. Antibiot.* **1971**, *24*, 722–723.
- (8) Spector, I.; Shochet, N. R.; Kashman, Y.; Groweiss, A. Latrunculins: Novel Marine Toxins That Disrupt Microfilament Organization in Cultured Cells. *Science* **1983**, *219*, 493.
- (9) Bubb, M. R.; Senderowicz, A. M.; Sausville, E. A.; Duncan, K. L.; Korn, E. D. Jasplakinolide, a Cytotoxic Natural Product, Induces Actin Polymerization and Competitively Inhibits the Binding of Phalloidin to F-Actin. *J. Biol. Chem.* **1994**, *269*, 14869–14871.
- (10) Holzinger, A.; Blaas, K. In *Cytoskeleton Methods and Protocols: Methods and Protocols*; Gavin, R. H., Ed.; Springer New York: New York, NY, 2016; pp 243–261.
- (11) Holzinger, A. In *Cytoskeleton Methods and Protocols*; Gavin, R. H., Ed.; Humana Press: Totowa, NJ, 2010; pp 71–87.
- (12) Fenteany, G.; Zhu, S. Small-Molecule Inhibitors of Actin Dynamics and Cell Motility. *Curr. Top. Med. Chem.* **2003**, *3*, 593–616.
- (13) Peterson, J. R.; Mitchison, T. J. Small Molecules, Big Impact: a History of Chemical Inhibitors and the Cytoskeleton. *Chem. Biol.* **2002**, *9*, 1275–1285.
- (14) Melak, M.; Plessner, M.; Grosse, R. Actin Visualization at a Glance. *J. Cell Sci.* **2017**, *130*, 525–530.
- (15) Lukinavicius, G.; Reymond, L.; D’Este, E.; Masharina, A.; Gottfert, F.; Ta, H.; Guther, A.; Fournier, M.; Rizzo, S.; Waldmann, H.; Blaukopf, C.; Sommer, C.; Gerlich, D. W.; Arndt, H.-D.; Hell, S. W.; Johnsson, K. Fluorogenic Probes for Live-Cell Imaging of the Cytoskeleton. *Nat. Methods* **2014**, *11*, 731–733.
- (16) Milroy, L.-G.; Rizzo, S.; Calderon, A.; Ellinger, B.; Erdmann, S.; Mondry, J.; Verveer, P.; Bastiaens, P.; Waldmann, H.; Dehmelt, L.; Arndt, H.-D. Selective Chemical Imaging of Static Actin in Live Cells. *J. Am. Chem. Soc.* **2012**, *134*, 8480–8486.
- (17) Stehn, J. R.; Haass, N. K.; Bonello, T.; Desouza, M.; Kottyan, G.; Treutlein, H.; Zeng, J.; Nascimento, P. R. B. B.; Sequeira, V. B.; Butler, T. L.; Allanson, M.; Fath, T.; Hill, T. A.; McCluskey, A.; Schevzov, G.; Palmer, S. J.; Hardeman, E. C.; Winlaw, D.; Reeve, V. E.; Dixon, L.; Weninger, W.; Cripe, T. P.; Gunning, P. W. A Novel Class of Anticancer Compounds Targets the Actin Cytoskeleton in Tumor Cells. *Cancer Res.* **2013**, *73*, 5169–5182.
- (18) Blanchoin, L.; Boujemaa-Paterski, R.; Sykes, C.; Plastino, J. Actin Dynamics, Architecture, and Mechanics in Cell Motility. *Physiol. Rev.* **2014**, *94*, 235–263.
- (19) Heng, Y.-W.; Koh, C.-G. Actin Cytoskeleton Dynamics and the Cell Division Cycle. *Int. J. Biochem. Cell Biol.* **2010**, *42*, 1622–1633.
- (20) Broichhagen, J.; Frank, J. A.; Trauner, D. A Roadmap to Success in Photopharmacology. *Acc. Chem. Res.* **2015**, *48*, 1947–1960.
- (21) Velema, W. A.; Szymanski, W.; Feringa, B. L. Photopharmacology: Beyond Proof of Principle. *J. Am. Chem. Soc.* **2014**, *136*, 2178–2191.
- (22) Pittolo, S.; Gómez-Santacana, X.; Eckelt, K.; Rovira, X.; Dalton, J.; Goudet, C.; Pin, J.-P.; Llobet, A.; Giraldo, J.; Llebaria, A.; Gorostiza, P. An Allosteric Modulator to Control Endogenous G Protein-Coupled Receptors with Light. *Nat. Chem. Biol.* **2014**, *10*, 813–815.
- (23) Borowiak, M.; Nahaboo, W.; Reynders, M.; Nekolla, K.; Jalinot, P.; Hasserodt, J.; Rehberg, M.; Delattre, M.; Zahler, S.; Vollmar, A.; Trauner, D.; Thorn-Seshold, O. Photoswitchable Inhibitors of Microtubule Dynamics Optically Control Mitosis and Cell Death. *Cell* **2015**, *162*, 403–411.
- (24) Hüll, K.; Morstein, J.; Trauner, D. In Vivo Photopharmacology. *Chem. Rev.* **2018**, *118*, 10710–10747.
- (25) Beharry, A. A.; Woolley, G. A. Azobenzene Photoswitches for Biomolecules. *Chem. Soc. Rev.* **2011**, *40*, 4422–4437.
- (26) Schönberger, M.; Althaus, M.; Fronius, M.; Claus, W.; Trauner, D. Controlling Epithelial Sodium Channels with Light Using Photoswitchable Amilorides. *Nat. Chem.* **2014**, *6*, 712.
- (27) Wegener, M.; Hansen, M. J.; Driessen, A. J. M.; Szymanski, W.; Feringa, B. L. Photocontrol of Antibacterial Activity: Shifting from UV to Red Light Activation. *J. Am. Chem. Soc.* **2017**, *139*, 17979–17986.
- (28) Tron, G. C.; Pirali, T.; Sorba, G.; Pagliai, F.; Busacca, S.; Genazzani, A. A. Medicinal Chemistry of Combretastatin A4: Present and Future Directions. *J. Med. Chem.* **2006**, *49*, 3033–3044.
- (29) Gaspari, R.; Prota, A. E.; Bargsten, K.; Cavalli, A.; Steinmetz, M. O. Structural Basis of *cis*- and *trans*-Combretastatin Binding to Tubulin. *Chem.* **2017**, *2*, 102–113.
- (30) Tannert, R.; Hu, T.-S.; Arndt, H.-D.; Waldmann, H. Solid-Phase Based Total Synthesis of Jasplakinolide by Ring-Closing Metathesis. *Chem. Commun.* **2009**, 1493–1495.
- (31) Doolittle, L. A.; Rosen, M. K.; Padrick, S. B. Measurement and Analysis of *in vitro* Actin Polymerization. *Methods Mol. Biol.* **2013**, *1046*, 273–293.
- (32) Kevenaar, J. T.; Hoogenraad, C. C. The Axonal Cytoskeleton: From Organization to Function. *Front. Mol. Neurosci.* **2015**, *8*, 44.
- (33) Mooren, O. L.; Galletta, B. J.; Cooper, J. A. Roles for Actin Assembly in Endocytosis. *Annu. Rev. Biochem.* **2012**, *81*, 661–686.
- (34) Gegenfurtner, F. A.; Zisis, T.; Al Danaf, N.; Schrimpf, W.; Kliesmete, Z.; Ziegenhain, C.; Enard, W.; Kazmaier, U.; Lamb, D. C.; Vollmar, A. M.; Zahler, S. Transcriptional Effects of Actin-Binding Compounds: The Cytoplasm Sets the Tone. *Cell. Mol. Life Sci.* **2018**, *75*, 4539–4555.
- (35) Olson, E. N.; Nordheim, A. Linking Actin Dynamics and Gene Transcription to Drive Cellular Motile Functions. *Nat. Rev. Mol. Cell Biol.* **2010**, *11*, 353–365.
- (36) Parmacek, M. S. Myocardin-Related Transcription Factors. *Circ. Res.* **2007**, *100*, 633–644.
- (37) Ellis-Davies, G. C. R. Caged Compounds: Photorelease Technology for Control of Cellular Chemistry and Physiology. *Nat. Methods* **2007**, *4*, 619–628.
- (38) Wu, Y. I.; Frey, D.; Lungu, O. I.; Jaehrig, A.; Schlichting, I.; Kuhlman, B.; Hahn, K. M. A Genetically Encoded Photoactivatable Rac Controls the Motility of Living Cells. *Nature* **2009**, *461*, 104–108.
- (39) Valon, L.; Marín-Llauradó, A.; Wyatt, T.; Charras, G.; Trepast, X. Optogenetic Control of Cellular Forces and Mechanotransduction. *Nat. Commun.* **2017**, *8*, 14396.
- (40) van Haren, J.; Charafeddine, R. A.; Ettinger, A.; Wang, H.; Hahn, K. M.; Wittmann, T. Local Control of Intracellular Microtubule Dynamics by EB1 Photodissociation. *Nat. Cell Biol.* **2018**, *20*, 252–261.

(41) Gao, L.; Kraus, Y.; Wranik, M.; Weinert, T.; Pritzl, S.; Meiring, J.; Bingham, R.; Olieric, N.; Akhmanova, A.; Lohmüller, T.; Steinmetz, M.; Thorn-Seshold, O. Photoswitchable Microtubule Inhibitors Enabling Robust, GFP-Orthogonal Optical Control Over the Tubulin Cytoskeleton. *bioRxiv*, July 27, 2019, DOI: 10.1101/716233.

(42) Singh, A.; Saha, T.; Begemann, I.; Ricker, A.; Nüsse, H.; Thorn-Seshold, O.; Klingauf, J. R.; Galic, M.; Matis, M. Polarized Microtubule Dynamics Directs Cell Mechanics and Coordinates Forces During Epithelial Morphogenesis. *Nat. Cell Biol.* **2018**, *20*, 1126–1133.

(43) Zenker, J.; White, M. D.; Templin, R. M.; Parton, R. G.; Thorn-Seshold, O.; Bissiere, S.; Plachta, N. A. Microtubule-Organizing Center Directing Intracellular Transport in the Early Mouse Embryo. *Science* **2017**, *357*, 925–928.

(44) Eguchi, K.; Taoufiq, Z.; Thorn-Seshold, O.; Trauner, D.; Hasegawa, M.; Takahashi, T. Wild-Type Monomeric α -Synuclein Can Impair Vesicle Endocytosis and Synaptic Fidelity via Tubulin Polymerization at the Calyx of Held. *J. Neurosci.* **2017**, *37*, 6043–6052.

(45) Müller-Deku, A.; Loy, K.; Kraus, Y.; Heise, C.; Bingham, R.; Ahlfeld, J.; Trauner, D.; Thorn-Seshold, O. Photoswitchable Microtubule Stabilisers Optically Control Tubulin Cytoskeleton Structure and Function. *bioRxiv*, September 22, 2019, DOI: 10.1101/778993.

(46) Pospich, S.; Kumpula, E.-P.; von der Ecken, J.; Vahokoski, J.; Kursula, I.; Raunser, S. Near-Atomic Structure of Jasplakinolide-Stabilized Malaria Parasite F-Actin Reveals the Structural Basis of Filament Instability. *Proc. Natl. Acad. Sci. U. S. A.* **2017**, *114*, 10636–10641.

(47) Merino, F.; Pospich, S.; Funk, J.; Wagner, T.; Küllmer, F.; Arndt, H.-D.; Bieling, P.; Raunser, S. Structural Transitions of F-Actin Upon ATP Hydrolysis at Near-Atomic Resolution Revealed by Cryo-EM. *Nat. Struct. Mol. Biol.* **2018**, *25*, 528–537.